Design and Activity of a Murine and Humanized Anti-CEACAM6 Single-Chain Variable Fragment in the Treatment of Pancreatic Cancer

Christopher J. Riley,[1] Kevin P. Engelhardt,[1] Jose W. Saldanha,[4] Wenqing Qi,[1] Laurence S. Cooke,[1] Yingting Zhu,[1] Satya T. Narayan,[1] Kishore Shakalya,[1] Kimiko Della Croce,[1] Ivan G. Georgiev,[1] Raymond B. Nagle,[1] Harinder Garewal,[2] Daniel D. Von Hoff,[3] and Daruka Mahadevan[1]

[1]Arizona Cancer Center; [2]Southern Arizona VA Medical Center, Tucson, Arizona; [3]TGen, Phoenix, Arizona; and [4]National Institute for Medical Research, London, United Kingdom

Abstract

Pancreatic ductal adenocarcinoma (PDA) is a lethal disease, with surgery being the only curative modality for localized disease, and gemcitabine with or without erlotinib remains the standard of therapy for unresectable or metastatic disease. CEACAM6 is overexpressed in human PDA independent of stage or grade and causes anoikis resistance when dysregulated. Because murine monoclonal antibody 13-1 possesses target-specific cytotoxicity in human PDA cell lines, we designed a humanized anti-CEACAM6 single-chain variable fragment (scFv) based on monoclonal antibody 13-1. PEGylation of the glycine-serine linker was used to enhance plasma half-life. These scFvs bound CEACAM6 with high affinity, exhibited cytotoxic activity, and induced dose-dependent poly(ADP-ribose) polymerase cleavage. Murine PDA xenograft models treated with humanized scFv alone elicited tumor growth inhibition, which was enhanced in combination with gemcitabine. Immunohistochemistry showed significant apoptosis, with inhibition of angiogenesis and proliferation, and preservation of the target. Collectively, our results have important implications for the development of novel antibody-based therapies against CEACAM6 in PDA. [Cancer Res 2009;69(5):1933–40]

Introduction

In 2007, pancreatic ductal adenocarcinoma (PDA) accounted for ~37,170 cancer cases, of which there were ~33,370 deaths, providing a dismal prognosis (1). This is attributable to a lack of early diagnosis and effective treatments. Most patients present with unresectable and/or metastatic PDA, with a median overall survival of 12 and 6 months, respectively (2). Therefore, the molecular basis of PDA is being intensely investigated in the hope of identifying disease mechanisms and associated therapeutic targets (3, 4). Genetic lesions linked to PDA have identified germline mutations in *KRAS, CDKN2A* (also known as *INK4a* or *ARF*), *BRCA2, MLH1, STK11* (also known as *LKB1*), *TP53*, and *SMAD4* (also known as *DPC4*; ref. 5), and a progression model similar to colon cancer has been postulated with the identification of a precursor lesion, pancreatic intraepithelial neoplasia (6–8). These lesions seem to acquire mutations in the above genes in a temporal sequence at progressive stages of pancreatic intraepithelial neoplasia (6). Genetically engineered mice have been established with the implicated mutated genes but do not completely recapitulate human PDA (9). A hallmark in PDA is the presence of a "desmoplastic reaction" due to proliferation of fibrotic tissue with an altered extracellular matrix (ECM) conducive to tumor growth and metastasis. Novel therapies targeting the desmoplastic reaction are required (3, 4), and CEACAM6 is one such target, expressed only in higher vertebrates (dogs and monkeys) and humans (10).

CEACAM6 (*CD66c*) is an integral member of the CEA family (CEACAM1, CEACAM5, CEACAM7, and CEACAM8) and is an important tumor-associated antigen (11). It is a cell surface glycoprotein composed of an extracellular region containing three immunoglobulin-like domains (344 residues; molecular weight ~35,200 daltons) and is linked to the plasma membrane via a glycophosphoinositol-anchor (12). CEACAM6 is capable of homophilic and/or heterophilic adhesion to other CEACAM family members (13). CEACAM6 is expressed on normal human epithelial and myeloid cells but the level of expression is 1 to 2 log lower compared with expression in malignant tissue (14). Several gene expression profiling studies on PDA cell lines (15, 16) and human PDA biopsy samples (17) have shown CEACAM6 to be 20- to 25-fold overexpressed compared with normal pancreatic ductal epithelial cells (15, 17). CEACAM6 is also overexpressed in several other epithelial carcinomas (colon, breast, ovarian, and non–small-cell lung cancers; refs. 14, 18).

Deregulated overexpression of CEACAM6 inhibits differentiation and apoptosis of cells when deprived of their anchorage to the ECM, a process known as anoikis (19). A small interfering RNA targeting CEACAM6 reversed anoikis resistance and inhibited the *in vivo* metastatic potential in a mouse xenograft model of PDA by enhancing caspase-3–mediated apoptosis (20). In BxPC-3 PDA cells, gene silencing of CEACAM6 markedly increased sensitivity to gemcitabine-mediated cytotoxicity (21). In a similar model, a maytansinoid (tubulin-interactive agent)–conjugated murine monoclonal antibody (mAb), but not unconjugated mAb, against CEACAM6 led to tumor growth inhibition (TGI) in a dose-dependent manner (22). Cynomolgus monkeys, when treated with the unconjugated or immunoconjugated mAb, showed a decrease in absolute neutrophil count 7 days after dosing, but only with the immunoconjugated group; no other toxicities were detected, and these effects were absent in the group treated with the unconjugated mAb. These results show that CEACAM6 is a potential therapeutic target for mAb therapy with a safe therapeutic index. We have designed and developed novel humanized single-chain

Requests for reprints: Daruka Mahadevan, Arizona Cancer Center, 1515 North Campbell Avenue, Tucson, AZ 85724. Phone: 520-626-4331; Fax: 520-626-2225; E-mail: dmahadevan@azcc.arizona.edu.

doi:10.1158/0008-5472.CAN-08-2707

variable fragments (scFv) antibody fragments based on murine mAb 13-1 (23), using *in silico* modeling methods. The novelty and uniqueness of this scFv-based therapeutic is that it promotes apoptosis without either cellular or humoral immune assistance. Furthermore, the PEGylated scFv enhances TGI alone and sensitizes with gemcitabine in mouse xenograft models of PDA. These results have important implications for the development of novel pancreatic cancer therapies.

Materials and Methods

Histopathology. Thirty human PDA biopsy samples were deparaffinized and microwaved for antigen retrieval, or if fixed frozen, the above step was omitted. Both types of sections were acetone-fixed and stained with α-NCA mAb (13-1, Kamiya) and processed using a mixture of anti-Ms and anti-Rb immunoglobulins. After rinsing, slides were incubated with an avidin-horseradish peroxidase reagent, rinsed, and incubated in 3,3′-diaminobenzidine. The slides were counterstained in hematoxylin. Mouse xenograft tumors (both control and treated) were divided in half and either snap-frozen or processed for paraffin embedding. Paraffin block sections were analyzed by immunohistochemistry for proliferation (*MKI67*, also known as *Ki-67*), angiogenesis (*PECAM1*, also known as *CD31*), and targeting (CEACAM6). The extent of apoptosis was estimated by H&E staining. Counting was done by summing the number of positively stained cells in five random fields under a microscope at ×20 magnification.

PDA cell lines. Ten human pancreatic cancer cell lines (CAPAN-2, CFPAC-1, Panc-1, AsPC-1, MiaPaCa-2, CAPAN-1, BxPC-3, Hs766T, Su.86.86, and HPAF-2) were grown in RPMI 1640 supplemented with 10% fetal bovine serum (Atlas Biologicals) in a CO_2 incubator. For Western blotting applications, cells were grown to ~75% confluence, pelletted via centrifugation, lysed with native lysis buffer, run on SDS-PAGE, transferred to nitrocellulose, and probed with the appropriate antibody. Native lysis buffer composition: 50 mmol/L HEPES, 150 mmol/L NaCl, 1% (v/v) Triton X-100, 5 mmol/L EDTA, 20 mmol/L NaF, 20 mmol/L $MgCl_2$, and 20 mmol/L $Na_4P_2O_7$, with Na_3VO_4 (1 mmol/L), phenylmethanesulfonylfluoride (1 mmol/L), and protease inhibitor cocktail (10 μL/10^7 cells; Sigma Aldrich) added immediately before use.

Mouse xenograft models. BxPC-3, HPAF-2, or Panc-1 cells (~10×10^6) were injected into the flank region of severe combined immunodeficiency mice to form small nodules (~60–100 mm^3). Treatment with unconjugated murine anti-CEACAM6 scFv or PEGylated humanized anti-CEACAM6 scFv [version 8 (V8)] was initiated when tumors reached >60 mm^3. Unconjugated scFv was given daily, i.p., for 4 wk. The PEGylated scFv was given twice a week for 4 wk via the same method. The primary end point was TGI compared with controls using the formula [$(\text{width})^2 \times \text{length}$] / 2. The secondary end point was effect of treatment on apoptosis, proliferation, angiogenesis, and continued expression of CEACAM6, evaluated by immunohistochemistry. Supernatant (medium) from BxPC-3 cells in culture as well as serum from BxPC-3 xenograft mice were collected and analyzed for shedding of CEACAM6 by Western blotting with mAb 13-1. The positive control was recombinant GST-CEACAM6 or BxPC-3 cell lysate.

Cell viability and apoptosis assays. BxPC-3, HPAF-2, and CAPAN-2 PDA cells were plated onto 96-well plates, such that cell confluency would reach ~80% by the end of the assay. After overnight incubation to allow for adhesion, cells were exposed to anti-CEACAM6 mAb 13-1 or scFv for 4 d. All studies were done in quadruplicate and were repeated three different times. After incubation, 20 μL of 2 mg/mL 3-(4,5-dimethylthiazol-2-yl)-2,5-diphenyltetrazolium bromide and 0.92 mg/mL phenazine methosulfate were added to each well and incubated for an additional 4 h; absorbance was read at 490 nm on a plate reader (Wallac Vector, Perkin-Elmer). Data were expressed as a percentage of survival, compared with controls, calculated from the absorbance and corrected for background. For apoptosis assays, PDA cells were treated with scFv at 10 and 20 μg/mL for 24 and 48 h, lysed, and analyzed by Western blotting to compare poly(ADP-ribose) polymerase (PARP) cleavage in treated cells and untreated controls (PARP and cleaved-PARP antibodies from Cell Signaling).

Humanization by design. mAb 13-1 V_L and V_H region sequence was characterized by mass spectroscopic peptide mapping and compared with that in the National Center for Biotechnology Information (NCBI) protein sequence database (no. JC5810 for V_L; no. PC4436 for V_H). For homology modeling and design (24) of scFv fragments, a PSI-BLAST search (NCBI) was conducted to identify the crystal structure(s) of a mouse mAb with the highest sequence similarity to the V_L and V_H of mAb 13-1. Sequence alignments of V_L and V_H domains of 1MCP (25) were done with the V_L and V_H of 13-1 in Clustal W. Molecular modeling of 13-1 V_L and V_H was done with 1MCP (Octane Silicon Graphics workstation) using Internal Coordinate Mechanisms and refined in Sybyl 6.9 (Tripos). A glycine-serine linker was constructed linking the V_L COOH terminus to the V_H NH_2 terminus (~33 Å) with a cysteine residue in the following order: GGGGSGGGGS (cys) GGGGS. The linker length of 16 residues was chosen to avoid oligomer formation. The cysteine residue was introduced into the linker because it is a potential site for PEGylation. The mouse scFv homology model and sequence was used to identify the best human acceptor for the V_L and V_H domains. The design was based on searching through the Kabat database (26) using the program FASTA (27) with analysis of the modeled structure using the program QUANTA (Accelrys, 2000). Care was taken to conserve the canonical forms and residues at the interface between the light and heavy chains. For V_H, the NCBI nonredundant database was searched with FASTA (27), and the modeled structure analyzed as above.

Gene synthesis, expression, purification, and PEGylation. We used a gene synthesis approach to construct the murine and nine humanized scFv versions. All 10 constructs were cloned into a pET25 expression vector with a COOH-terminally located hexa-histidine tag. DNA sequencing confirmed the authenticity of these constructs. Five scFv constructs (the murine version and humanized V1, V2, V7, and V8) were expressed

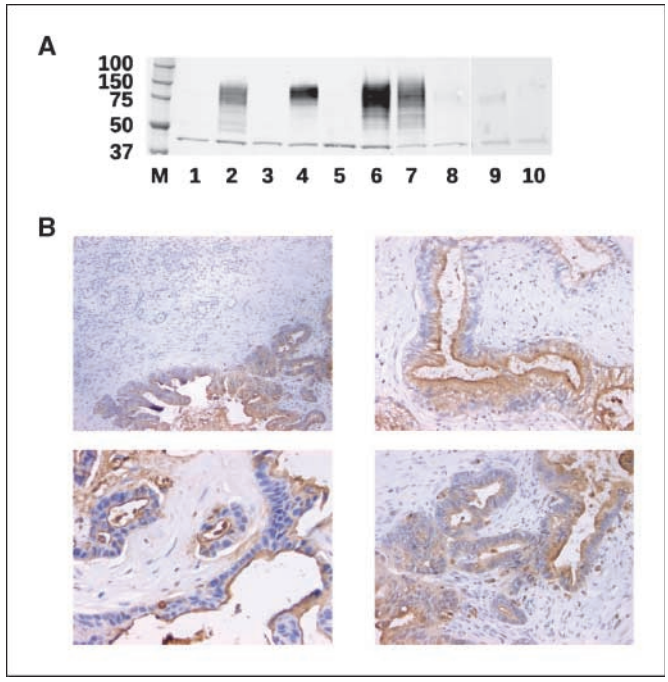

Figure 1. *A,* Western blotting showing CEACAM6 expression in 10 human pancreatic cancer cell lines (*M,* marker; *1,* CAPAN-2; *2,* CFPAC-1; *3,* Panc-1; *4,* AsPC-1; *5,* MiaPaCa-2; *6,* CAPAN-1; *7,* BxPC-3; *8,* Hs766T; *9,* Su.86.86; *10,* HPAF-2). CEACAM6 migrates at 90 kDa due to variable glycosylation, and the band at 45 kDa is the β-actin control. *B,* immunohistochemical staining of four representative PDA patient biopsy samples with the murine anti-CEACAM6 mAb 13-1. The intense dark brown staining of the malignant pancreatic ductal surface epithelium is evident (apical and basal staining).

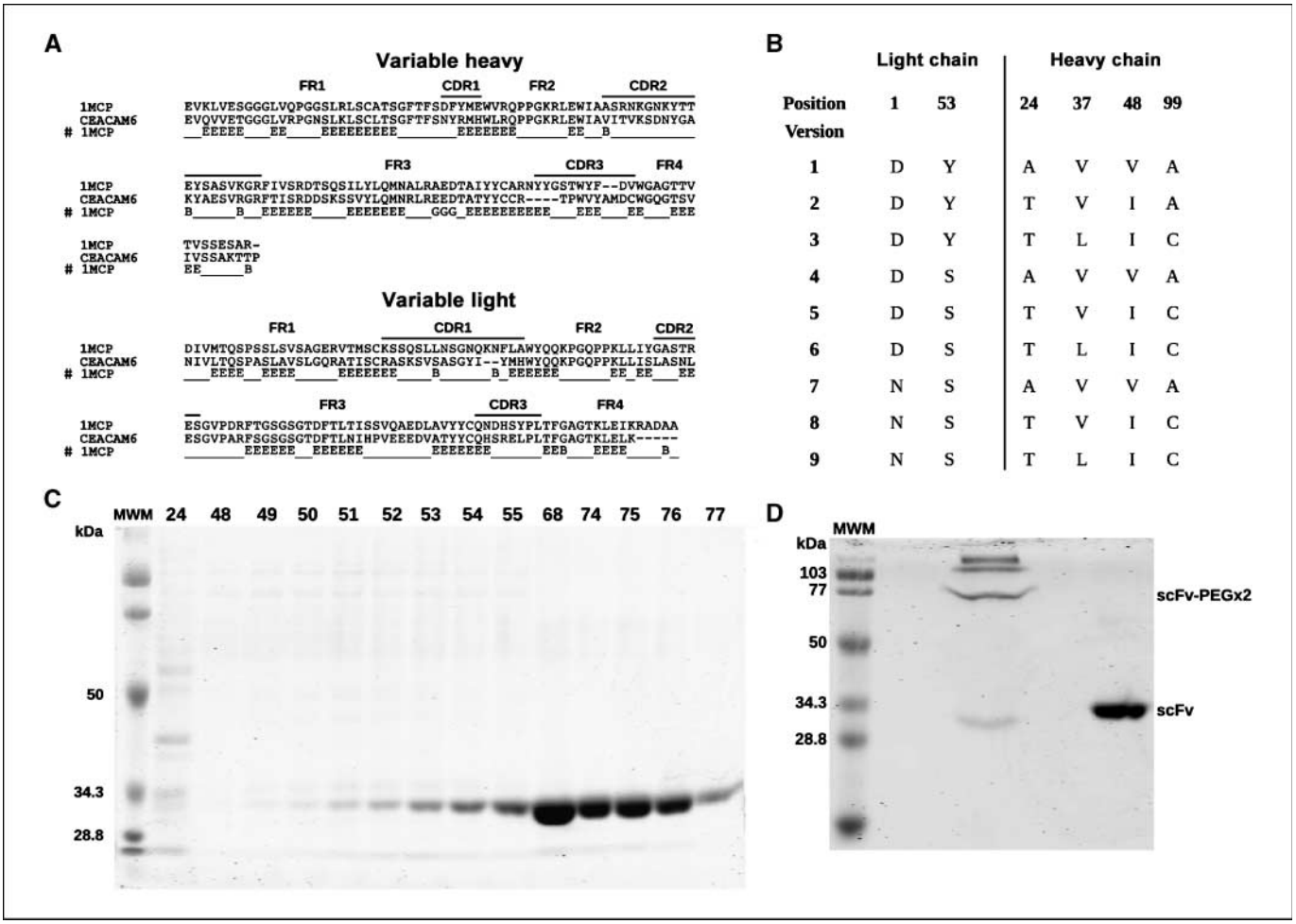

Figure 2. *A,* the structure-based sequence alignment of the murine anti-CEACAM6 V_H and V_L chains with the V_H and V_L of 1MCP. *B,* amino acid differences between the nine humanized versions of the anti-CEACAM6 scFv. *C,* Coomassie-stained fractions collected from purification on a nickel affinity column (AKTA FPLC) of humanized scFv anti-CEACAM6-V8. *D,* Coomassie-stained PEGylated anti-CEACAM6-V8. The molecular weight shift is ~40 kDa in the PEGylated version.

in BL21 (DE3) PlysS competent bacteria; inclusion bodies were isolated, denatured in 8 mol/L urea buffer, and refolded by drop-wise introduction to Tris-HCl refolding buffer (pH 7.4). Refolded scFvs were concentrated to 0.3 mg/mL and buffer-exchanged using a PD-10 desalting column into a cysteine-reducing buffer (100 mmol/L $NaPO_4$, 100 mmol/L imidazole, 2 mmol/L DTT, 2 mmol/L EDTA, pH 7.0). Samples were rocked gently for 2 h at room temperature and buffer-exchanged into PEGylation buffer (100 mmol/L $NaPO_4$, 100 mmol/L imidazole, 2 mmol/L EDTA, pH 6.0), then placed in a reaction apparatus under argon gas. PEG-maleimide 20 kDa (Nektar) was added to the mixture and the reaction continued for 2 h under a constant argon gas stream. Once the reaction was complete, the samples were stored at −4°C (13). Western blotting confirms protein PEGylation due to a 20- or 40-kDa shift in molecular weight, to a molecular weight of 40 or 60 kDa depending on one- or two-site PEGylation (one site is located in the linker, and the other in the COOH terminus of the V_H domain).

Homology models, protein-protein docking, and binding studies. The three immunoglobulin-like ECDs of human CEACAM6 (NCBI no. P40199) were homology-modeled based on the crystal structure of rat NCAM (residues 1–291; pdb:1QZ1; ref. 28) using "Modeller."[5] Rat NCAM was identified and chosen for use by structure-based sequence analysis (3D-PSSM)[6] and using sequence alignment in ClustalW.[7] The model was energy-minimized (Powell method), and Procheck v.3.5.4[8] evaluated the correctness of this refined/energy minimized model. Protein-protein docking of human CEACAM6 ECD (1–291) with mouse or humanized anti-CEACAM6 scFv (V1–V9) was done in ClusPro.[9] Electrostatic energy (kcal/mol), desolvation energy (kcal/mol), and theoretical affinity were calculated using FastContact.[10]

Immunoblotting. For *in vitro* studies for humanized scFv (V1, V2, V7, and V8), Western blotting and immunoprecipitation were used with the PDA cell lines (BxPC-3, HPAF-2, and CAPAN-2). For immunoprecipitation, scFv was added to cell lysates (1 μg/μL total protein content, calculated via bicinchoninic acid assay; proteins lysed with native lysis buffer as discussed previously) and incubated with rocking at 4°C overnight, then precipitated with 20 μL of Ni-NTA Superflow beads (Qiagen) under the same conditions. Beads were pelletted via centrifugation, washed thrice with cold PBS, and protein was removed by the addition of Laemmli loading buffer and heating to 95°C for 2 min followed by centrifugation; supernatant was removed and stored at −20°C. For Western blotting, cell lysates were

[5] http://salilab.org/modeller

[6] http://www.sbg.bio.ic.ac.uk/~3dpssm/index2.html
[7] http://www.ebi.ac.uk/Tools/clustalw2/index.html
[8] http://www.biochem.ucl.ac.uk/~roman/procheck/procheck.html
[9] http://nrc.bu.edu/cluster
[10] http://structure.pitt.edu/servers/fastcontact

prepared after treatment with scFv for 6 h. SDS-PAGE and Western blotting were done with anti-CEACAM6 antibody (Abcam). For immunoblotting, the murine mAb to CEACAM6 (13-1; Kamiya) and an anti–β-actin control were also used.

Statistical analysis. Statistical analysis was computed using STATA software (StataCorp LP). *P* values were calculated using ANOVA with Bonferroni correction, calculating a lower critical α level to allow for multiple testing.

Results

CEACAM6 is overexpressed in human PDA. Relative to normal pancreatic tissue, ~50% PDA cell lines (Fig. 1*A*) and >90% of patient biopsies overexpressed CEACAM6 irrespective of stage or grade of disease (Fig. 1*B*). Of the 10 human PDA cell lines (CAPAN-2, CFPAC-1, Panc-1, AsPC-1, MiaPaCa-2, CAPAN-1, BxPC-3, Hs766T, Su.86.86, and HPAF-2) evaluated by Western blotting with the murine mAb 13.1, five were overexpressers (CFPAC-1, AsPC-1, CAPAN-1, BxPC-3, and HPAF-2), two were low expressers (Hs766T and Su.86.86), and three were nonexpressers (CAPAN-2, Panc-1, and MiaPaCa-2). The protein migrates at a molecular weight of 60 to 90 kDa due to variable glycosylation patterns. Of the 30 patient biopsies, 26 (>90%) showed intense cell surface staining of neoplastic pancreatic ductal cells whereas surrounding normal tissues were not stained, clearly delineating tumor cells and normal pancreatic tissue. Cell culture medium and serum from mouse BxPC-3 xenograft tumors showed that CEACAM6 is not shed from the cell surface (data not shown). Hence, CEACAM6 is a feasible target for development of a therapeutic mAb and may have additional utility in identifying micrometastatic sites via imaging during initial workup for potential surgical intervention and to follow disease status during therapy.

Humanization by design. The V_L design was based on the human sequence 163.15 (Kabat database ID 047292; ref. 29). The first three residues of this sequence were changed to the most common residues found in human sequences (i.e., Asp-Ile-Val). Humanized V1 is a straight graft of the CEACAM6 complementarity-determining regions (CDR) into the human frameworks. Humanized V2 changes the human Tyr at position 49 to the Ser found in the CEACAM6 V_L chain. From the model, Ser49 is the most prominent framework residue in the binding site and binding affinity may be evaluated by mutation. The model shows that it might interact with Met100a in the heavy chain of CDR-H3. It can also interact with nearby CDR residues in the V_L chain. The NH_2 terminus is occasionally important in binding antigen (30); hence, V3 changes the human Asp at position 1 to the Asn found in the CEACAM6 light chain. From the model, this Asn interacts with

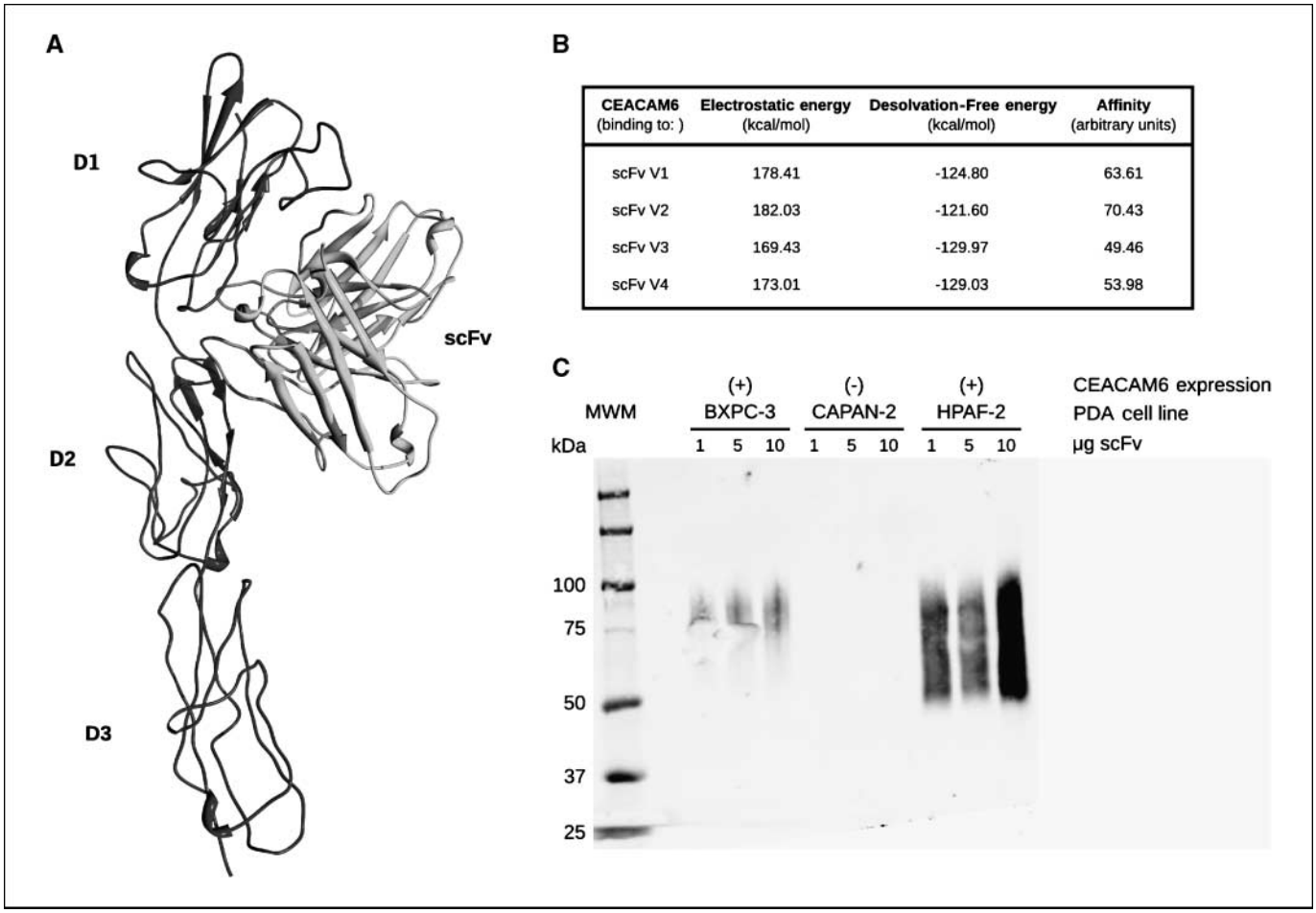

CEACAM6 (binding to:)	Electrostatic energy (kcal/mol)	Desolvation-Free energy (kcal/mol)	Affinity (arbitrary units)
scFv V1	178.41	-124.80	63.61
scFv V2	182.03	-121.60	70.43
scFv V3	169.43	-129.97	49.46
scFv V4	173.01	-129.03	53.98

Figure 3. *A,* protein-protein docking shows that the anti-CEACAM6 scFv binds to CEACAM6 immunoglobulin-like D1-2 and disrupts immunoglobulin-like D1-D1 homophilic dimer formation. *B,* theoretical binding energy and affinity for four scFv versions with CEACAM6. *C,* Western blotting with CEACAM6 [9A6] of immunoprecipitation products using anti-CEACAM6-V7 (1, 5, or 10 μg) with three PDA cell line lysates.

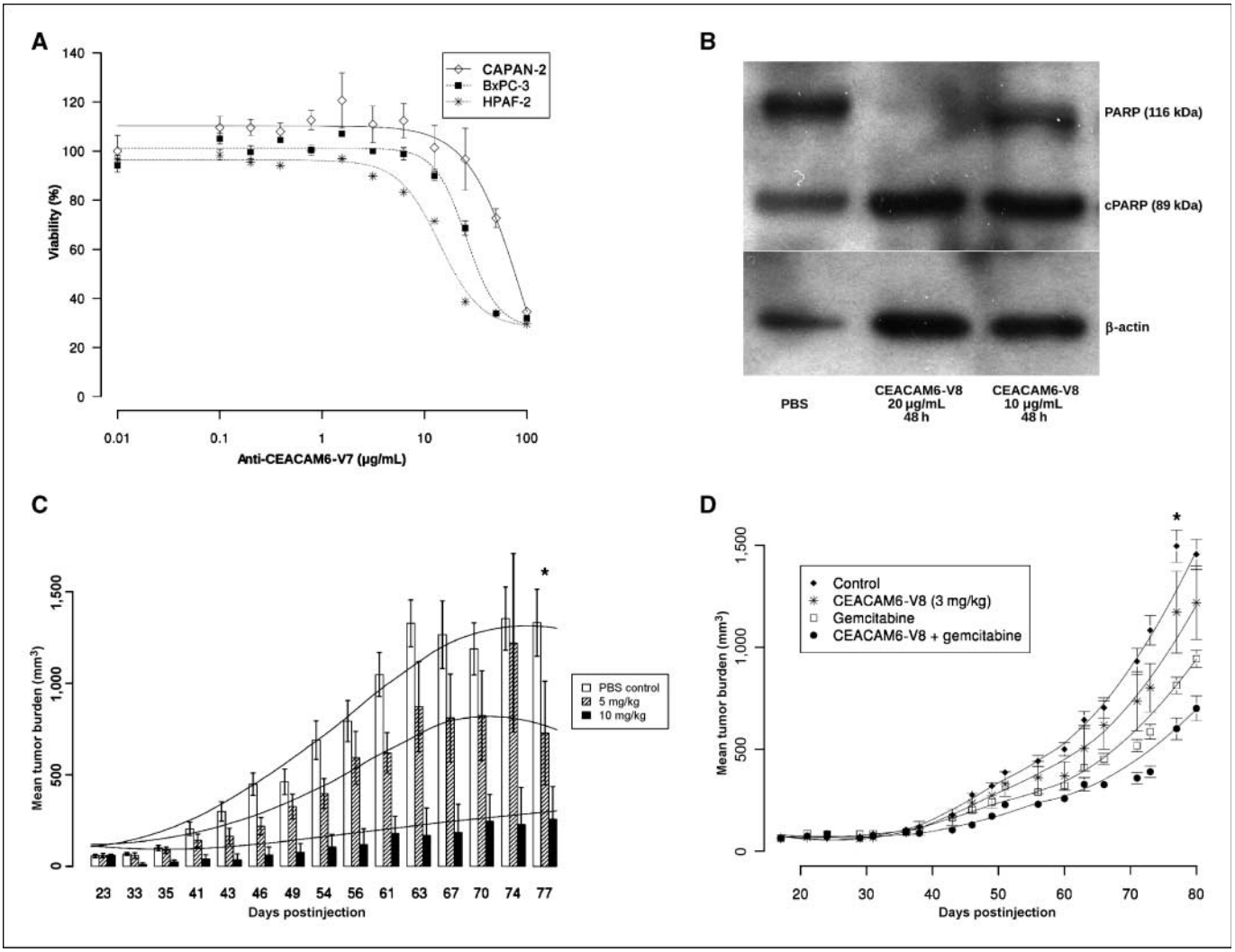

Figure 4. *A,* 3-(4,5-dimethylthiazol-2-yl)-2,5-diphenyltetrazolium bromide assay showing that anti-CEACAM6-V7 antibody fragment is efficient at killing two different CEACAM6$^+$ pancreatic cell lines; *bars* SE. *B,* Western blot showing PARP cleavage following treatment of HPAF-2 cells with anti–CEACAM6-V8. *C,* mouse scFv given i.p. is effective in delaying tumor growth in a dose-dependent manner (n=8); *bars*, SE. *, P = 0.015, control versus 10 mg/kg anti–CEACAM6 mouse scFv. *D,* mean tumor burden in a mouse model treated twice weekly with gemcitabine with or without PEGylated anti–CEACAM6-V8 (n=8); *bars*, SE. *, P = 0.031, control versus germcitabine alone; P = 0.001, control versus gemcitabine plus CEACAM6-V8.

Pro95 in CDR-L3 and with Lys27 in CDR-L1 and may also interact with Glu61 in CDR-H2. Version 3 only has two back mutations (Fig. 2*A*).

The V_H design was based on the human sequence AAC51024 (NCBI accession no. 1791061; ref. 31). It is notable that all three CDRs are the same length as 13-1. Humanized V1 is a straight graft of the CEACAM6 CDRs into these human frameworks. Version 2 changes the human Ala24 to Thr found in the V_H CEACAM6 and, similarly, Val48 to Ile. Thr24 is a canonical residue for CDR-H1 and possibly interacts with Phe27 and Phe29. Ile48 is a common back mutation in humanization experiments and, from the model, seems to support the conformation of CDR-H2. Version 3 mutates the unusual Cys93 to Ala and Val37 to Leu. Leu37 is a residue at the light/heavy interface and was kept murine. Cys93 in the model seems to be interacting with Tyr99. There is a possibility that Cys93 may be forming a disulfide bridge with Cys102 in CDR-H3 (32), although this is unlikely from the model or is contributing to a metal binding site (Fig. 2*A*). Because the CDRs in both the V_L and V_H regions are identical in the chosen human acceptors, the only residues that require mutations are in the framework regions at the base of the CDR loops (V_L-1, 53; V_H-24, 37, 48, 99). Humanized V4 to V9 were designed based on these mutational changes (Fig. 2*B*).

Purification and PEGylation. Recombinant scFv (V_L-ggggs-ggggscggggs-V_H) versions (murine and humanized V1, V2, V7, and V8) yielded 5 to 10 mg/L of bacterial culture, with >95% purity (AKTA FPLC), and were refolded into PBS (Fig. 2*C*). All four humanized versions were PEGylated successfully and run as a 70-kDa band on SDS-PAGE due to a shift in the molecular weight by 40 kDa, as there are two PEGylation sites for V8: one in the linker and the other in the COOH terminus of the V_H domain (Fig. 2*D*). The PEGylated scFv is stable in PBS at 4°C.

Anti-CEACAM6 scFv disrupts immunoglobulin-like D1-D1 homophilic dimer formation. Computational protein-protein docking of the three immunoglobulin-like ECDs showed that domain 1 (D1) formed the optimal homophilic dimer based on electrostatic and desolvation-free energies. These data correlate well with structure-function and mutational data conducted on

CEACAM6 (13, 33). Moreover, docking studies of scFv Vs CEACAM6 ECD indicated that the best binder based on engagement of all CDRs from both the V_L and V_H domains was scFv V7, followed by V8, V1, and V2, respectively (Fig. 3*A* and *B*). The scFv versions bind to immunoglobulin-like D1-2 and thereby disrupt immunoglobulin-like D1-D1 homophilic interactions. These results correlate with the estimates of direct electrostatic and desolvation interaction-free energy (Fig. 3*B*) for the four humanized scFv versions. The specificity of the scFv (V1, V2, V7, and V8) for CEACAM6 was shown by immunoprecipitation and Western blotting analysis of two CEACAM6-expressing PDA cell lines (BxPC-3 and HPAF-2) compared with non–CEACAM6-expressing CAPAN-2 cells (Fig. 3*C*).

Anti-CEACAM6 scFv decreases tumor cell viability and increases TGI in a PDA mouse model. mAb 13-1 promoted a target-specific decrease in tumor cell viability in CAPAN-1 and HPAF-2 with an IC_{50} of 1 to 10 μg/mL, whereas no change in cell viability was observed for Panc-1 and MiaPaCa-2 cells (data not shown). Murine scFv also promoted a decrease in PDA cell viability with an IC_{50} of 0.01 to 0.5 μg/mL (data not shown). Humanized scFv V1, V2, V7, and V8 (un-PEGylated) similarly decreased cell viability in a target-specific manner with an IC_{50} in the range 5 to 10 μg/mL (Fig. 4*A*), similar to that observed for mAb 13-1, and promoted PARP cleavage in a dose-dependent manner (Fig. 4*B*).

To evaluate efficacy, several mouse PDA xenograft models were conducted. The first study evaluated the murine scFv (5 and 10 mg/kg) in severe combined immunodeficiency mice bearing BxPC-3 xenografts, which showed a significant dose-dependent TGI of >50% (Fig. 4*C*). Because scFvs have a $t_{1/2}$ of ~30 minutes (13), the persistent TGI observed is remarkable. The second study evaluated humanized PEGylated scFv (V8) at 3 and 6 mg/kg with and without gemcitabine. The TGI was modest at both dose levels at ~25%, but sensitizes with gemcitabine with a TGI of >50% (6 mg/kg, Fig. 4*D*; data not shown). The tumors harvested at the end of the study showed persistent CEACAM6 expression in all treated arms (scFv plus gemcitabine, scFv alone, and gemcitabine alone) following immunohistochemistry, suggesting the possibility that continuous treatment with the scFv or combination with gemcitabine was feasible. The third study evaluated treatment with PEGylated humanized scFv (V8) at 3 and 6 mg/kg given twice a week for 3 weeks; tumors were harvested and analyzed by immunohistochemistry for CEACAM6 (Fig. 5*A*), apoptosis and angiogenesis (Fig. 5*B*), and proliferation (Fig. 5*C*). There were four tumors per arm that showed a significant dose-dependent increase in apoptosis (3-fold by morphology), decrease in angiogenesis (20–60%) and proliferation (Ki-67; 25–48%), but persistence of the target CEACAM6 (~60%).

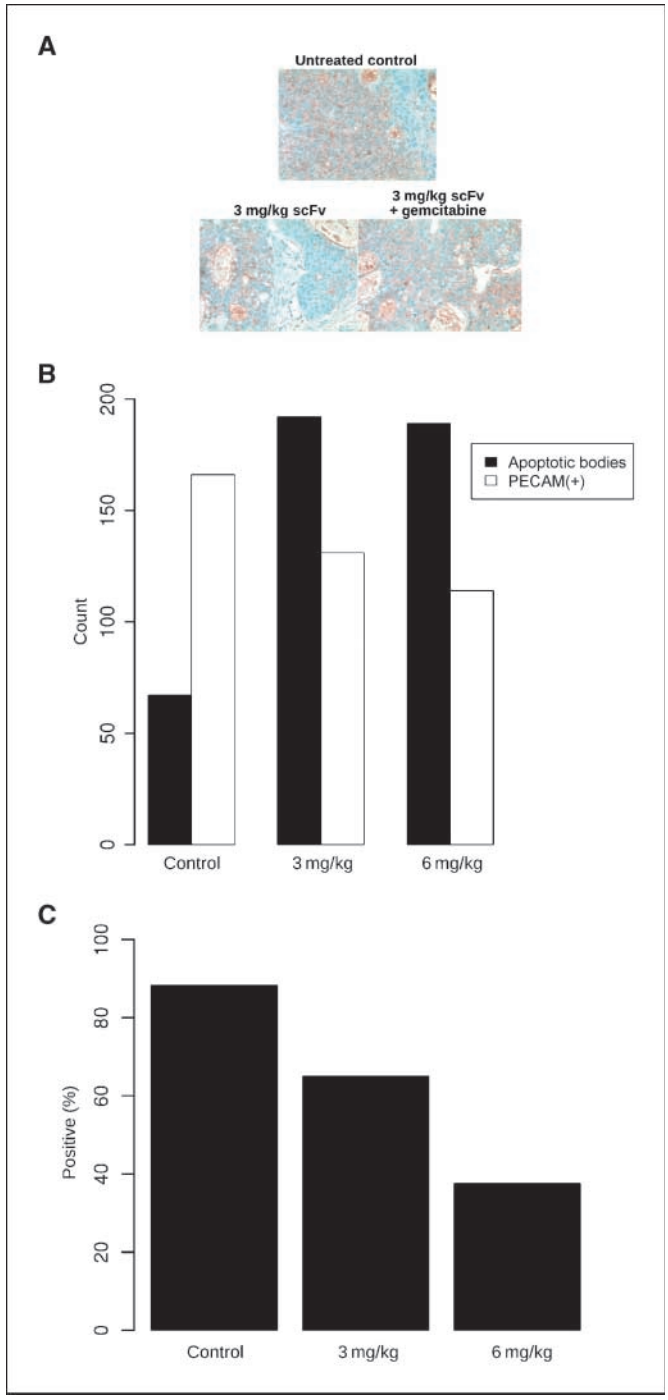

Figure 5. *A,* immunohistochemical staining of mouse tumor tissue treated with anti–CEACAM6-V8 and stained for CEACAM6 [9A6]. *B,* numbers of apoptotic bodies and PECAM(+) cells counted on slides from anti-CEACAM6-V8–treated mice. *C,* percentage positivity for Ki67 from anti-CEACAM6-V8–treated mice.

Discussion

Deregulated cell surface overexpression of CEACAM6 was observed in >50% of human hematologic and solid tumors. CEACAM6 is a well-validated antibody target in gastrointestinal malignancies such as colorectal cancer (14, 34) and PDA (3, 21). Overexpression of CEACAM6 inhibits differentiation and apoptosis of cells when deprived of their anchorage to the ECM, a process known as anoikis (Greek for "homelessness"), which accompanies malignant transformation (19). Cross-linking CEACAM6 in a BxPC-3 mouse xenograft model with an anti-CEACAM6 mAb (By114) induces cytoplasmic accumulation but with no associated TGI. However, a secondary saporin-conjugated IgG does induce cytotoxicity via caspase-3–mediated apoptosis with associated TGI (21).

Mouse mAb 13-1 directed against CEACAM6 markedly reduced PDA cell viability in a target-specific manner with an IC_{50} of 1 to 10 μg/mL, independent of antibody-dependent cellular cytotoxicity and complement-dependent cytotoxicity. Furthermore, CEACAM6 was not detected in either the culture medium

or in serum samples from BxPC-3 xenograft mice, indicating a lack of shedding from the cell surface. Therefore, we designed a murine and nine humanized scFv versions using a structure-based *in silico* method to evaluate activity without additional activity (antibody-dependent cellular cytotoxicity and complement-dependent cytotoxicity). Recombinant murine and humanized versions (1, 2, 7, 8) bound CEACAM6 specifically, markedly reduced PDA cell viability (IC_{50}, 5–50 μg/mL), and exhibited associated dose-dependent PARP cleavage (10 and 20 μg/mL). The non-PEGylated mouse scFv showed 50% to 70% TGI in a BxPC-3 murine xenograft model in a dose-dependent manner (5 and 10 mg/kg). Subsequently, humanized PEGylated (35) scFv V8 alone at 3 mg/kg showed TGI of ~25%, but with the addition of gemcitabine showed TGI of >50%.

The novel and unique characteristic of these humanized anti-CEACAM6 scFv antibody fragments lies in their ability to specifically induce targeted tumor cell apoptosis without dependence on antibody-dependent cellular cytotoxicity, complement-dependent cytotoxicity, or conjugation with a cytotoxic agent. We postulate that this ability originates from their mode and high affinity of binding to CEACAM6, which enhances the disruption of D1-D1 homophilic dimer with consequent functional inhibition. Moreover, deletion of the Fc-fragment from mAb 13-1 in the design prevents additional toxicity mediated by antibody-dependent cellular cytotoxicity and complement-dependent cytotoxicity to normal tissue without compromising efficacy. Finally, the PEGylated anti-CEACAM6 scFv is soluble, has a longer half-life, and likely penetrates tumors more effectively compared with a full antibody molecule.

A pharmacodynamic study using immunohistochemistry of BxPC-3 xenograft mice tumors treated with humanized PEGylated scFv V8 at two different doses (3 and 6 mg/kg) twice a week for 3 weeks showed that CEACAM6 continued to be expressed on tumor cells despite an increase in apoptosis (apoptotic bodies as well as cleaved caspase-3) and a decrease in proliferation (Ki-67) and angiogenesis (PECAM). Taken together, the data implicate that CEACAM6 continues to provide a survival benefit to PDA cells, and therefore, increasing the dose and duration of scFv therapy is likely to further enhance TGI. Furthermore, there is an anti-CEACAM6 scFv dose-dependent promotion of apoptosis with an associated decrease in proliferation and angiogenesis. Therefore, in conclusion, this study shows for the first time that a mouse and/or a humanized scFv alone directed against CEACAM6 promotes targeted killing of PDA cells independent of antibody-dependent cellular cytotoxicity and complement-dependent cytotoxicity. The fact that an anti-CEACAM6 scFv sensitized with gemcitabine provides a rationale for combination therapy for patients with PDA.

Disclosure of Potential Conflicts of Interest

No potential conflicts of interest were disclosed.

Acknowledgments

Received 7/15/2008; revised 11/17/2008; accepted 12/24/2008; published OnlineFirst 02/24/2009.

Grant support: NIH grant CA23074 to Arizona Cancer Center and Specialized Programs of Research Excellence in Gastrointestinal Cancer grant CA95060-03.

The costs of publication of this article were defrayed in part by the payment of page charges. This article must therefore be hereby marked *advertisement* in accordance with 18 U.S.C. Section 1734 solely to indicate this fact.

We thank Drs. David Bearss and L.H. Li for their contributions to target discovery and mass spectroscopic analysis. Immunohistochemical data were generated by the Tissue Acquisition and Cellular/Molecular Analysis Shared Service core and Experimental Mouse Shared Service at the Arizona Cancer Center.

This article is dedicated to Stephen R. Smith, whose fight against pancreatic cancer was heroic, and dedication to this project, inspirational.

References

1. Jemal A, Siegel R, Ward E, Murray T, Xu J, Thun MJ. Cancer statistics, 2007. CA Cancer J Clin 2007;57:43–66.
2. Von Hoff DD, Mahadevan D, Bearss DJ. New developments in the treatment of patients with pancreatic cancer. Clin Oncol Updates 2001;4:1–15.
3. Mahadevan D, Von Hoff, DD. Tumor-stroma cross talk in pancreatic adenocarcinoma. Mol Cancer Ther 2007;6:1186–97.
4. Engelhardt K, Riley C, Cooke LS, Mahadevan D. Monoclonal antibody therapies targeting pancreatic ductal adenocarcinoma. Curr Drug Discov Technol 2006;3:231–43.
5. Jaffee EM, Hruban RH, Canto M, Kern SE. Focus on pancreas cancer. Cancer Cell 2002;2:25–8.
6. Bardeesy N, DePinho RA. Pancreatic cancer biology and genetics. Nat Rev Cancer 2002;2:897–909.
7. Cubilla AL, Fitzgerald PJ. Morphological patterns of primary nonendocrine human pancreas carcinoma. Cancer Res 1975;35:2234–48.
8. Klein WM, Hruban RH, Klein-Szanto AJ, Wilentz RE. Direct correlation between proliferative activity and dysplasia in pancreatic intraepithelial neoplasia (PanIN): additional evidence for a recently proposed model of progression. Mod Pathol 2002;15:441–7.
9. Hingorani SR, Petricoin EF, Maitra A, et al. Preinvasive and invasive ductal pancreatic cancer and its early detection in the mouse. Cancer Cell 2003;4:437–50.
10. Singer BB, Scheffrahn I, Heymann R, Sigmundsson K, Kammerer R, Obrink B. Carcinoembryonic antigen-related cell adhesion molecule 1 expression and signaling in human, mouse, and rat leukocytes: evidence for replacement of the short cytoplasmic domain isoform by glycosylphosphatidylinositol-linked proteins in human leukocytes. J Immunol 2002;168:5139–46.
11. Barnett T, Goebel SJ, Nothdurft MA, Elting JJ. Carcinoembryonic antigen family: characterization of cDNAs coding for NCA and CEA and suggestion of nonrandom sequence variation in their conserved loop-domains. Genomics 1988;3:59–66.
12. Hefta SA, Paxton RJ, Shively JE. Sequence and glycosylation site identity of two distinct glycoforms of nonspecific cross-reacting antigen as demonstrated by sequence analysis and fast atom bombardment mass spectrometry. J Biol Chem 1990;265:8618–26.
13. Oikawa S, Sugiyama M, Kuroki M, Kuroki M, Nakazato H. Extracellular N-domain alone can mediate specific heterophilic adhesion between members of the carcinoembryonic antigen family CEACAM6 and CEACAM8. Biochem Biophys Res Commun 2000;278:564–8.
14. Schölzel S, Zimmermann W, Schwarzkopf G, Grunert F, Rogaczewski B, Thompson J. Carcinoembryonic antigen family members CEACAM6 and CEACAM7 are differentially expressed in normal tissues and oppositely deregulated in hyperplastic colorectal polyps and early adenomas. Am J Pathol 2000;156:595–605.
15. Han H, Bearss DJ, Browne LW, Calaluce R, Nagle RB, Von Hoff DD. Identification of differentially expressed genes in pancreatic cancer cells using cDNA microarray. Cancer Res 2002;62:2890–6.
16. Ryu B, Jones J, Blades NJ, et al. Relationships and differentially expressed genes among pancreatic cancers examined by large-scale serial analysis of gene expression. Cancer Res 2002;62:819–26.
17. Iacobuzio-Donahue CA, Maitra A, Olsen M, et al. Exploration of global gene expression patterns in pancreatic adenocarcinoma using cDNA microarrays. Am J Pathol 2003;162:1151–62.
18. Blumenthal RD, Leon E, Hansen HJ, Goldenberg DM. Expression patterns of CEACAM5 and CEACAM6 in primary and metastatic cancers. BMC Cancer 2007;7:2.
19. Ordonez C, Screaton RA, Ilantzis C, Stanners CP. Human carcinoembryonic antigen functions as a general inhibitor of anoikis. Cancer Res 2000;60:3419–24.
20. Duxbury MS, Hiromichi I, Zinner MJ, Ashley SW, Whang EE. CEACAM6 gene silencing impairs anoikis resistance and *in vivo* metastatic ability of pancreatic adenocarcinoma cells. Oncogene 2004;23:465–73.
21. Duxbury MS, Ito H, Benoit E, Waseem T, Ashley SW, Whang EE. A novel role for carcinoembryonic antigen-related cell adhesion molecule 6 as a determinant of gemcitabine chemoresistance in pancreatic adenocarcinoma cells. Cancer Res 2004;64:3987–93.
22. Strickland LA, Risser P, Verbeke C, Polakis P, Koeppen H. Evaluation of efficacy and toxicity of CEACAM6 targeted immunotherapy in pancreatic ductal adenocarcinoma. AACR Annual Meeting, April 2005, Anaheim, California. Abstract no. 4195.
23. Saldanha JW, Della Croce K, Vankayalapati H, Georgiev I, Nagel R, Mahadevan D. A humanized anti-CEACAM6 mAb targeting pancreatic adenocarcinoma demonstrates potent *in vitro* and *in vivo* activity. AACR Annual Meeting, March 2004, Orlando, Florida. Abstract 2180.
24. Saldanha JW. Molecular engineering I: humanization. In: Dubel S, editor. Handbook of therapeutic antibodies, volume 1. Weinheim: Wiley-VCH; 2007.
25. Satow Y, Cohen GH, Padlan EA, Davies DR.

Phosphocholine binding immunoglobulin Fab McPC603. An X-ray diffraction study at 2.7 A. J Mol Biol 1986;190: 593–604.
26. Johnson G, Wu TT. Kabat database and its applications: future directions. Nucleic Acids Res 2001;29:205–6.
27. Pearson WR. Flexible sequence similarity searching with the FASTA3 program package. Methods Mol Biol 2000;132:185–219.
28. Soroka V, Kolkova K, Kastrup JS, et al. Structure and interactions of NCAM Ig1-2-3 suggest a novel zipper mechanism for homophilic adhesion. Structure 2003;11: 1291–301.
29. Coomber DW, Hawkins NJ, Clark MA, Ward RL Generation of anti-p53 Fab fragments from individuals with colorectal cancer using phage display. J Immunol 1999;163:2276–83.
30. Kolbinger F, Saldanha J, Hardman N, Bendig MM. Humanization of a mouse anti-human IgE antibody: a potential therapeutic for IgE-mediated allergies. Protein Eng 1993;6:971–80.
31. Glas AM, Nottenburg C, Milner EC. Analysis of rearranged immunoglobulin heavy chain variable region genes obtained from a bone marrow transplant (BMT) recipient. Clin Exp Immunol 1997;107:372–80.
32. Akashi S, Kato K, Torizawa T, et al. Structural characterization of mouse monoclonal antibody 13-1 against a porphyrin derivative: identification of a disulfide bond in CDR-H3 of Mab 13-1. Biochem Biophys Res Commun 1997;240:566–72.
33. Kuroki M, Abe H, Imakiirei T, et al. Identification and comparison of residues critical for cell-adhesion activities of two neutrophil CD66 antigens, CEACAM6 and CEACAM8. J Leukoc Biol 2001;70:543–50.
34. Jantscheff P, Terracciano L, Lowy A, et al. Expression of CEACAM6 in resectable colorectal cancer: a factor of independent prognostic significance. J Clin Oncol 2003; 21:3638–46.
35. Yang K, Basu A, Wang M, et al. Tailoring structure-function and pharmacokinetic properties of single-chain Fv proteins by site-specific PEGylation. Protein Eng 2003;16:761–70.